

Spectroscopic Evidences for Strong Hydrogen Bonds with Selenomethionine in Proteins

*V. Rao Mundlapati^{1,2}, Dipak Kumar Sahoo^{1,2}, Sanat Ghosh³, Umesh Kumar Purame^{2,4},
Shubhant Pandey^{2,4}, Rudresh Acharya^{2,4}, Nitish Pal^{1,2,5}, Prince Tiwari^{1,2,6} and Himansu S.
Biswal^{1,2*}*

¹*School of Chemical Sciences, National Institute of Science Education and Research
(NISER), PO- Bhimpur-Padanpur, Via-Jatni, District- Khurda, PIN - 752050, Bhubaneswar,
India*

²*Homi Bhabha National Institute, Training School Complex, Anushakti Nagar, Mumbai
400094, India*

³*Tata Institute of Fundamental Research, Homi Bhabha Road, Mumbai 400005, India*

⁴*School of Biological Sciences, National Institute of Science Education and Research
(NISER), Institute of Physics Campus, Bhubaneswar 751 005, India*

⁵*Current Affiliation: Institute for Physical Chemistry II, Ruhr-University Bochum, 44780
Bochum, Germany.*

⁶*Current Affiliation: Department of Chemistry and Applied Biosciences, ETH Zurich, HCI D
325, CH-8093 Zurich, Switzerland.*

* Corresponding Author's E-mail: himansu@niser.ac.in, Phone No: - +91-674-2494 185/186

Experimental Methods: The solid samples (H-bond donors: NPAA and 2-PY) are vaporized by thermal heating to 80-100°C. About 0.2 -0.5% pre-mixture of H-bond acceptors (DMSe and DMS) in helium are used for the complex formation Both the H-bond donors and acceptors are entertained in supersonic jet expansion and cooled down to their zero point vibrational energy level. The supersonic-jet cooling (~10-20 K) has many advantages. It reduces spectral congestion significantly that helps to identify and assign conformation-specific infrared spectra, in the form of well-separated narrow vibronic bands. During the pre-expansion and expansion H-bonded complexes are formed and skimmed prior to entering the ionization chamber of the linear time-of-flight spectrometer.¹⁻⁴ The complexes are then studied using high resolution IR and UV laser spectroscopy. UV excitation spectra are recorded with mass-selective resonant two-photon ionisation (R2PI) spectroscopy while the single- conformation-specific IR spectra are obtained by IR/UV double resonance spectroscopy.

Computational Methods: The optimized structures of the monomers and H-bonded complexes are obtained at RI-B97-D/def2-TZVPP levele of theory. The IR spectra of the H-bonded complexes are also computed at the level of theory. The scaled harmonic frequencies obtained from the calculations are helpful to assign experimental IR spectra to specific conformations. The H-bond energies are estimated at the CCSD(T)/aug-cc-pVDZ level of theory. The natural bond orbital (NBO) analysis⁵ provides the donor-acceptor pair-wise interaction energies (E_{DA}). The NBO-EDA energies are computed at MP2/aug-cc-pVDZ. The existences of H-bonds are further supported by non-covalent interaction (NCI) analyses⁶ using the wave functions of the optimized structures at MP2/aug-cc-pvDZ. The atomic charges and esp are calculated at M06-2X/aug-cc-pVDZ level. Gaussian09⁷Turbomole 6.5⁸, NCI-PLOT⁶, and NBO-6.0⁹ are employed to carry out all the computations.

PDB Structure Analysis: The protein structure coordinates were retrieved from the RCSB website, which were satisfying the following criteria: structure resolved by X-ray crystallography at less than 2.5 Å resolution, comprising of Se (Mse: selenomethionine) and with less than 30% sequence identity among the proteins. This parametric selection results in the acquisition of 4472 protein dataset (non-redundant). REDUCE¹⁰ program was used to optimally compute the hydrogen atom positions in each amino acid for each PDB file. After predicting the H atom position in PDB coordinates, we used in-house programs written in C language to identify the hydrogen bonds defined by Selenium atom as acceptor. In our dataset of 4472 protein structures, we have observed 24641 Mse (~6 Mse/protein) which account for

4334 H-bonds i.e. roughly one out of every six Mse is involved in H-bond formation or every protein in this dataset on an average forms at least one Se centered H-bonds (SeCHBs). Out of observed 4334 H-bond interactions, 2342 are main-chain-NH $\bullet\bullet$ Se H-bonds and 1992 from side-chain-NH $\bullet\bullet$ Se H-bonds.

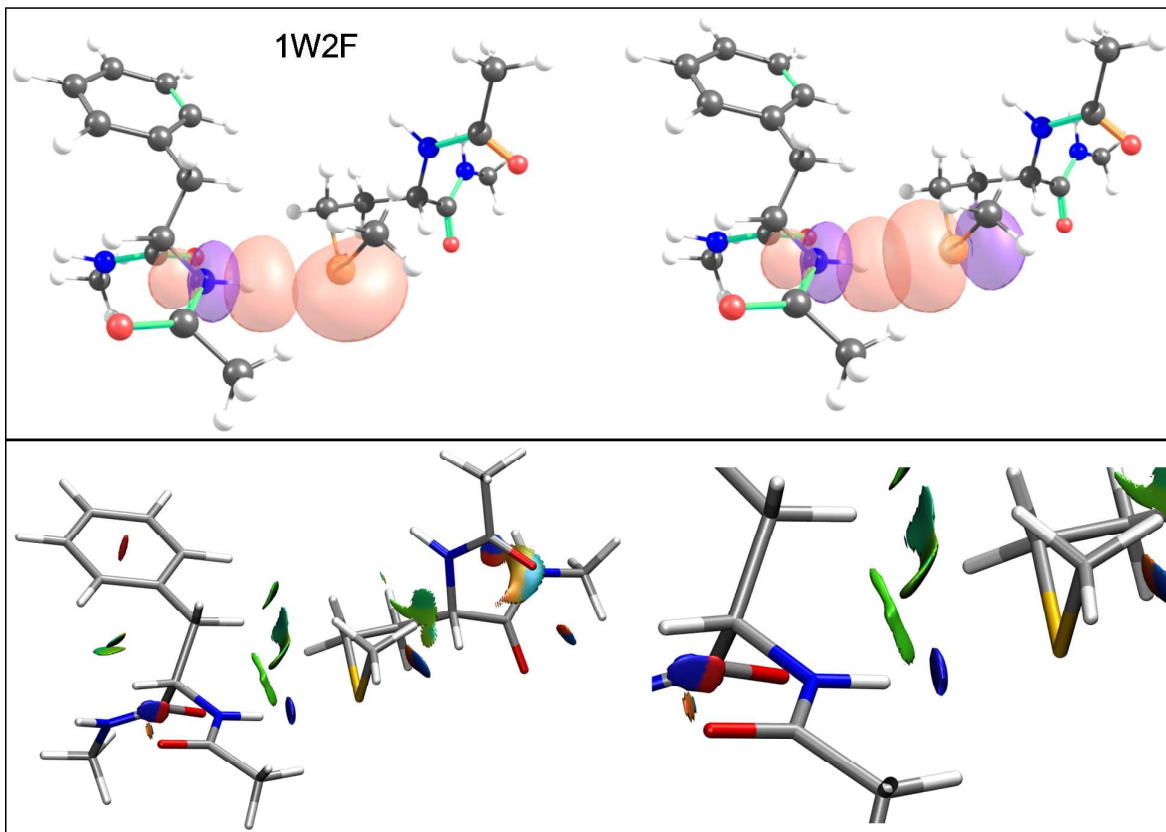


Figure S1. Amide-N-H H \cdots Se hydrogen bond observed in human inositol 1,4,5-trisphosphate 3-kinase (PDB: 1w2f, Resolution: 1.8 Å), characterized by

Upperpanel: overlap of s- and p-type Se lone pair and N-H σ^* orbitals: (d) phosphoethanolamine N-methyltransferase (PDB: 4krg, Resolution: 1.8 Å). The plots of the reduced density gradient (s) versus the sign of the second eigen value of the electron-density Hessian matrix (λ_2) times electron density ($\text{sign}(\lambda_2)\rho$) for (e) 1w2f and (f) 4krg with the bond critical point (BCP) of amide-N-H H \cdots Se hydrogen bond indicated.

Lower Pannel: colored isosurfaces of the reduced electron density gradient (3D-NCI-plot), following the NCI-plot topological analysis of the electron density at the MP2/aug-cc-pVDZ.

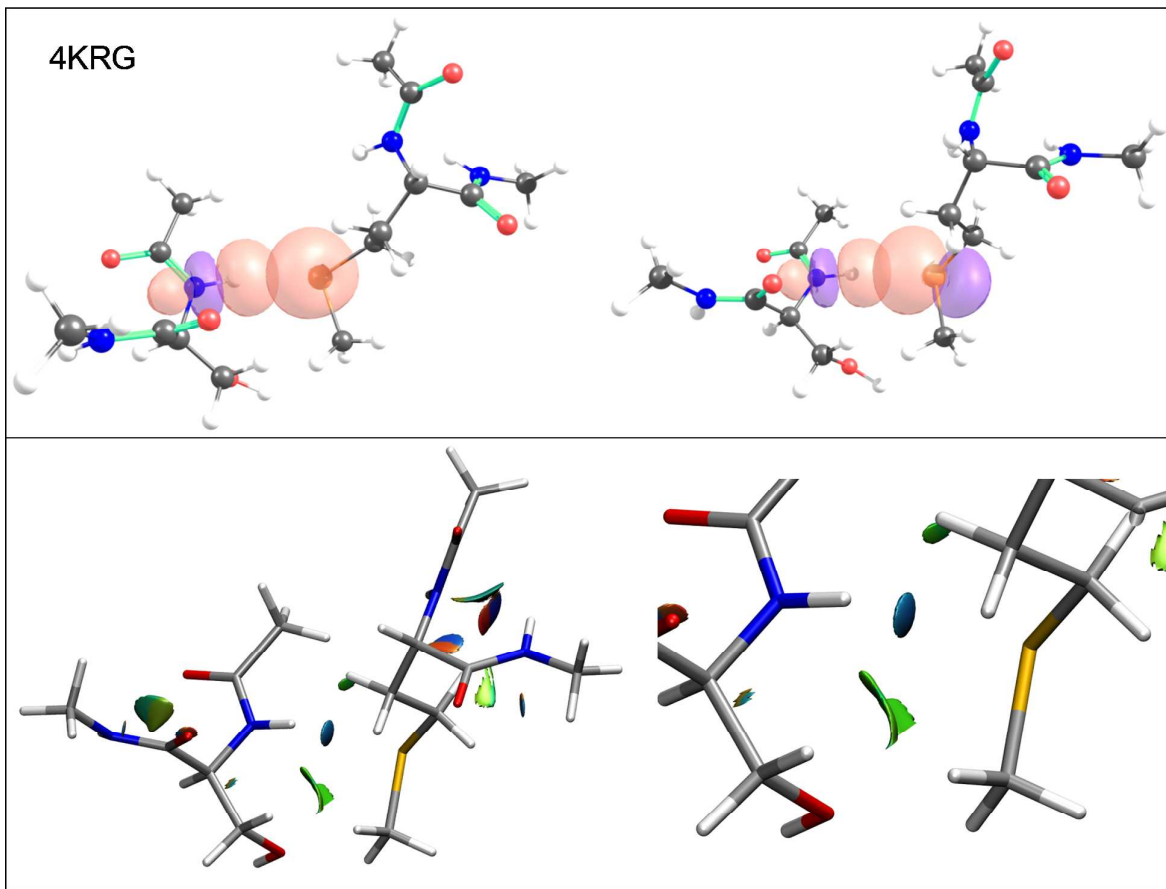


Figure S2. Amide-N-H H...Se hydrogen bond observed in phosphoethanolamine N-methyltransferase (PDB:4krg, Resolution: 1.8 Å), characterized by

Upper panel: overlap of s- and p-type Se lone pair and N-H σ^* orbitals:

Lower panel: colored isosurfaces of the reduced electron density gradient (3D-NCI-plot), following the NCI-plot topological analysis of the electron density at the MP2/aug-cc-pVDZ.

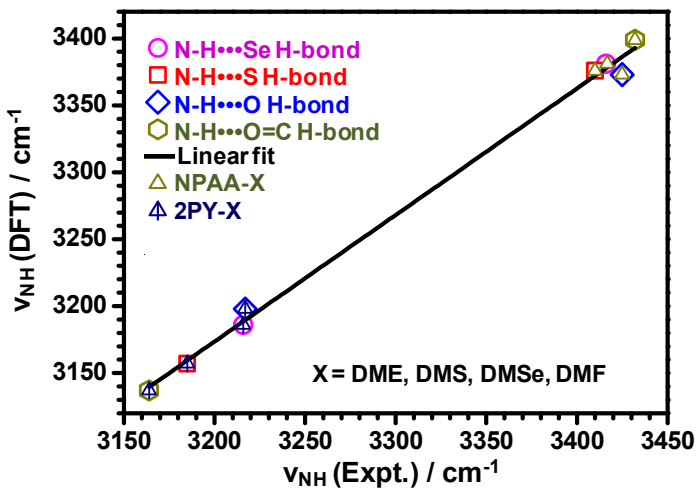


Figure S3. Linear correlation plot between vibrational frequencies estimated by DFT (ν_{NH} - DFT) and experimental N-H stretching frequencies (ν_{NH} - Expt.). The fitted equation, $\nu_{\text{NH}}(\text{Expt.}) = 0.9868 \times \nu_{\text{NH}}(\text{DFT}) + 11$ is used to estimate experimental N-H stretching frequencies (ν_{NH} - Expt.) of NPAA-DMTe, 2PY-DMTe and NMFA-DMTe amide-N-H \cdots Te H-bond complexes.

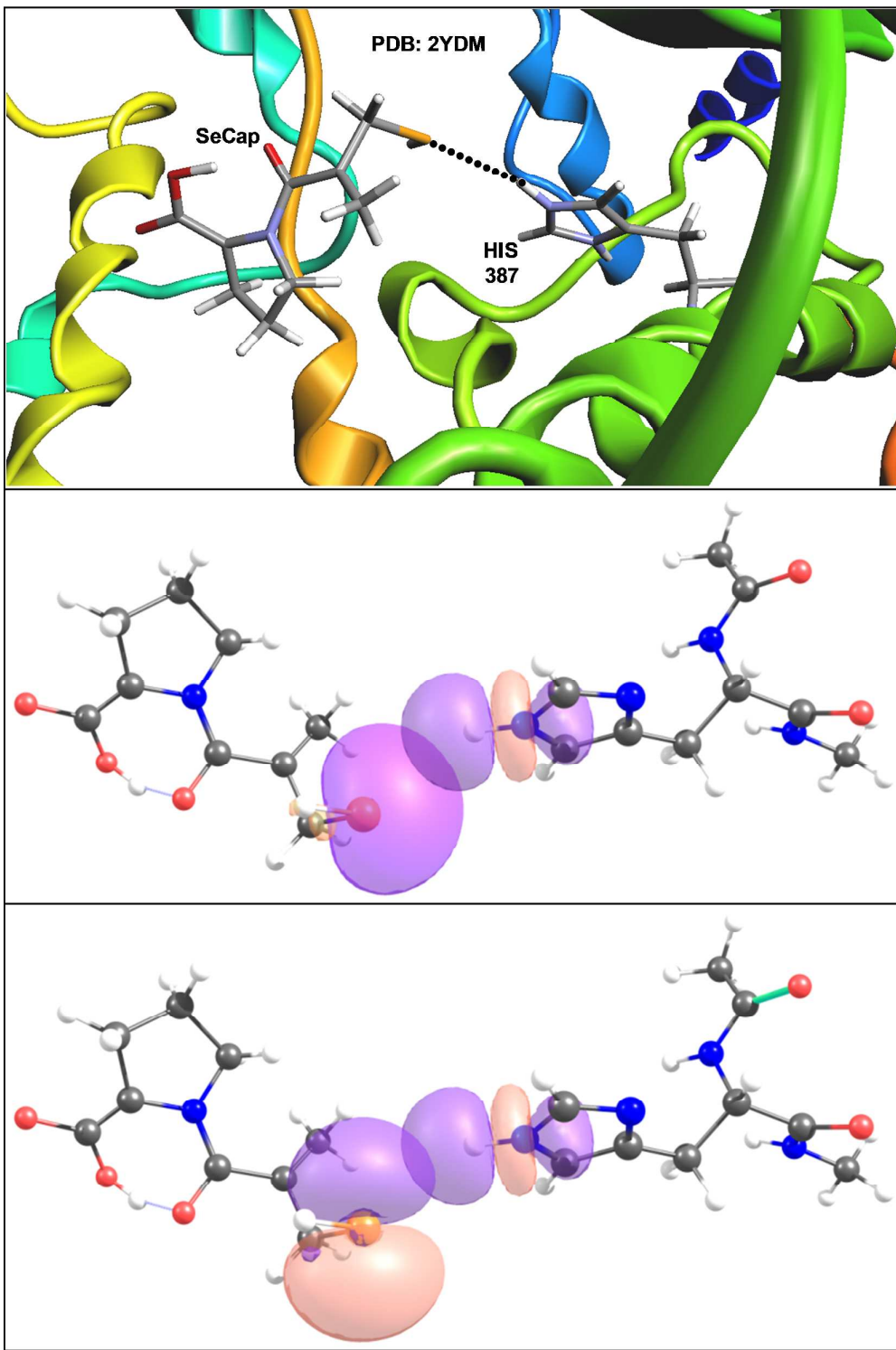


Figure S4. N-H H \cdots Se hydrogen bond observed in angiotensin-I converting enzyme in complex with a selenium analogue of captopril (PDB:2ydm, Resolution: 2.4 Å), characterized by overlap of s- and p-type Se lone pair and N-H σ^* orbitals:

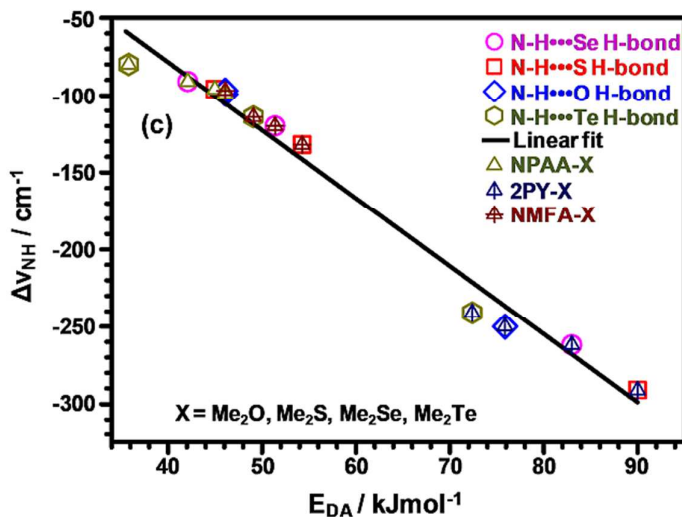


Figure S5: Linear correlation plot between donor-acceptor interaction energies (E_{DA}) and red shift of N-H stretching frequencies. The NBO calculation and NCI-plot topological analysis of the electron density were performed at the MP2/aug-cc-pVDZ level of theory.

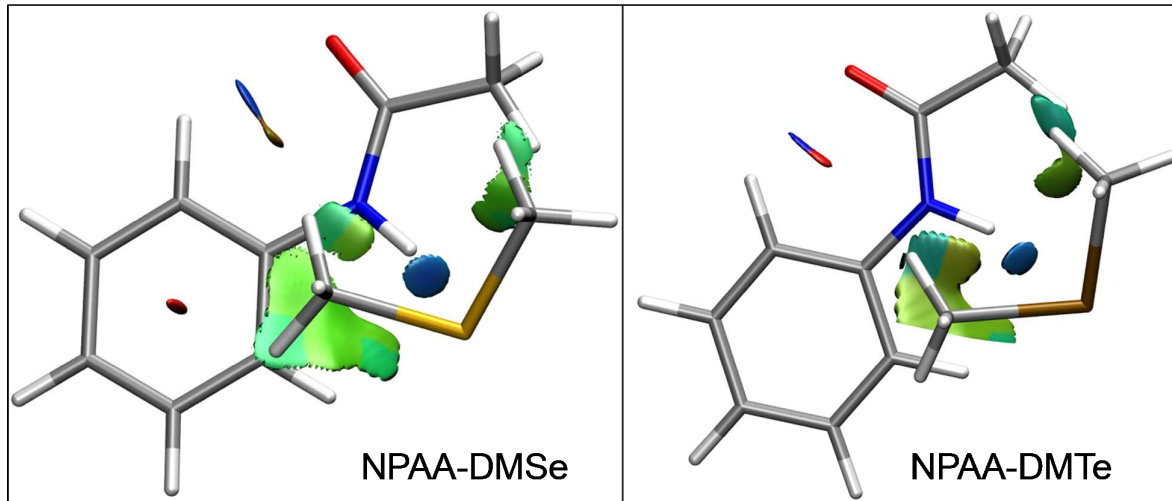


Figure S6. Primary N-H \cdots Se/Te H-bonds and secondary C-H \cdots Se/Te/ π H-bonds in NPAA-DMSe/DMTe complexes as revealed by colored isosurfaces of the reduced electron density gradient (3D-NCI-plot), following the NCI-plot topological analysis of the electron density at the MP2/aug-cc-pVDZ.

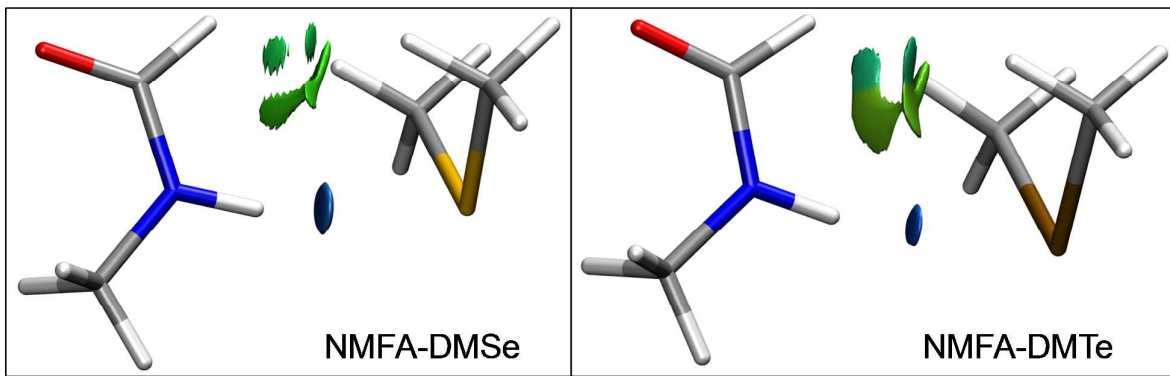


Figure S7. Primary N-H \cdots Se/Te H-bonds and secondary C-H \cdots S/Te H-bonds in NMFA-DMSe/DMTe complexes as revealed by colored isosurfaces of the reduced electron density gradient (3D-NCI-plot), following the NCI-plot topological analysis of the electron density at the MP2/aug-cc-pVDZ.

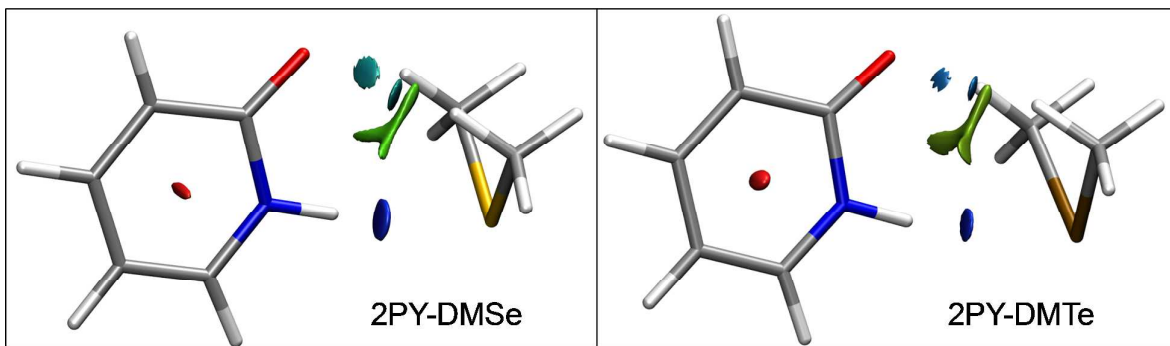


Figure S8. Primary N-H \cdots S/Te H-bonds and secondary C-H \cdots Se/Te/O H-bonds in 2PY-DMSe/DMTe complexes as revealed by colored isosurfaces of the reduced electron density gradient (3D-NCI-plot), following the NCI-plot topological analysis of the electron density at the MP2/aug-cc-pVDZ.

Table S1: Computed binding energy (D_0 in kJ/mol) at CCSD(T)/aug-cc-pVDZ, red shift of N-H stretching frequency ($\Delta\nu$ in cm^{-1}), and donor-acceptor interaction energies (E_{DA} in kJ/mol) for N-H \cdots Y (Y= O, S, Se, and Te) and N-H \cdots O=C H-bond complexes.

H-bond Type	NPAA-X (trans-amide)			2PY-X (cis-amide)			NMFA-X (trans-amide)		
	D_0	$\Delta\nu(\text{NH})$	E_{DA}	D_0	$\Delta\nu(\text{NH})$	E_{DA}	D_0	$\Delta\nu(\text{NH})$	E_{DA}
N-H \cdots O (X=DME)	39.2	-99	46.1	44.9	-250	75.9	27.2	-97	46.1
N-H \cdots S (X=DMS)	40.6	-96	45.0	49.0	-291	90.0	28.0	-132	54.3
N-H \cdots Se (X=DMSe)	41.2	-91	42.1	50.4	-262	83.0	29.5	-120	51.4
N-H \cdots Te (X=DMTe)	41.7	-80	35.8	46.1	-241	72.4	25.8	-114	49.1
N-H \cdots O=C (X=DMF)	55.1	-73	28.0	57.8	-311	101	32.1	-123	50.0

Table S2: Atomic polarizabilities of DME

Atom Type	$\mu_x 0$	$\mu_y 0$	$\mu_z 0$	μ_x	μ_y	μ_z	α_{xx}	α_{yy}	α_{zz}	α_{avg}	
H	0.184362	-0.691771	-0.000127	0.181708	-0.700959	-0.002553	2.65	9.19	2.43	4.76	
N	0.254464	-0.301769	0.000235	0.253182	-0.303475	-0.002911	1.28	1.71	3.15	2.04	
C	-0.001397	-0.133409	-0.000065	-0.003598	-0.134245	-0.003410	2.20	0.84	3.35	2.13	
H	-0.519603	-0.796576	0.000004	-0.526503	-0.805158	-0.002552	6.90	8.58	2.56	6.01	
O	-1.781202	2.056876	-0.000140	-1.793811	2.048626	-0.004507	12.61	8.25	4.37	8.41	
C	0.242644	0.175753	-0.000109	0.239962	0.175185	-0.000420	2.68	0.57	0.31	1.19	
H	-0.199904	0.580878	0.869344	-0.202283	0.575748	0.863640	2.38	5.13	5.70	4.40	
H	-0.197495	0.578538	-0.871186	-0.199895	0.573422	-0.876944	2.40	5.12	5.76	4.42	
H	0.833209	-0.396206	0.002039	0.819652	-0.397823	0.000143	13.56	1.62	1.90	5.69	
Total		-1.184921	1.072313	-0.000005	-1.231585	1.031321	-0.029514	46.66	40.99	29.51	39.05

Table S3: Atomic polarizability in a. u. of DMS

Atom Type	$\mu_x 0$	$\mu_y 0$	$\mu_z 0$	μ_x	μ_y	μ_z	α_{xx}	α_{yy}	α_{zz}	α_{avg}	
S	0.000004	-2.273088	-0.000078	-0.005598	-2.291524	-0.011644	5.60	18.44	11.57	11.87	
C	-0.488963	0.234390	0.000107	-0.493056	0.233383	-0.000585	4.09	1.01	0.69	1.93	
H	0.055098	0.611867	0.948974	0.051410	0.606018	0.942912	3.69	5.85	6.06	5.20	
H	-0.881520	-0.647680	-0.000475	-0.896109	-0.650148	-0.002705	14.59	2.47	2.23	6.43	
H	0.055597	0.612569	-0.948678	0.051909	0.606715	-0.954771	3.69	5.85	6.09	5.21	
C	0.489022	0.234339	-0.000619	0.484922	0.233332	-0.001311	4.10	1.01	0.69	1.93	
H	-0.057017	0.614160	0.947491	-0.060676	0.608295	0.941446	3.66	5.87	6.04	5.19	
H	-0.053706	0.610335	-0.950121	-0.057395	0.604496	-0.956229	3.69	5.84	6.11	5.21	
H	0.881520	-0.647676	0.003348	0.867028	-0.650143	0.001118	14.49	2.47	2.23	6.40	
Total		0.000034	-0.650784	-0.000051	-0.057565	-0.699577	-0.041768	57.60	48.79	41.72	49.37

Table S4: Atomic polarizability in a. u. of DMSe

Atom Type	$\mu_x 0$	$\mu_y 0$	$\mu_z 0$	μ_x	μ_y	μ_z	α_{xx}	α_{yy}	α_{zz}	α_{avg}	
Se	0.000001	-2.527474	-0.000115	-0.007855	-2.548069	-0.015475	7.86	20.59	15.36	14.60	
C	0.537443	0.327471	-0.000381	0.532224	0.325502	-0.001207	5.22	1.97	0.83	2.67	
H	-0.067455	0.624884	-0.984022	-0.071337	0.617913	-0.990442	3.88	6.97	6.42	5.76	
H	0.959979	-0.635822	0.002579	0.943995	-0.637875	0.000133	15.98	2.05	2.45	6.83	
H	-0.070100	0.627780	0.981920	-0.073960	0.620787	0.975561	3.86	6.99	6.36	5.74	
C	-0.537519	0.327336	-0.000074	-0.542726	0.325365	-0.000900	5.21	1.97	0.83	2.67	
H	0.067628	0.625066	0.984046	0.063735	0.618098	0.977667	3.89	6.97	6.38	5.75	
H	-0.959914	-0.635831	-0.002167	-0.976012	-0.637885	-0.004614	16.10	2.05	2.45	6.87	
H	0.069922	0.627653	-0.981862	0.066046	0.620661	-0.988264	3.88	6.99	6.40	5.76	
Total		-0.000015	-0.638936	-0.000076	-0.065890	-0.699503	-0.047542	65.88	56.57	47.47	56.64

Table S5: Atomic polarizability in a. u. of DMTe

Atom Type	$\mu_x 0$	$\mu_y 0$	$\mu_z 0$	μ_x	μ_y	μ_z	α_{xx}	α_{yy}	α_{zz}	α_{avg}	
Te	0.000090	-2.601407	0.002568	-0.012080	-2.628034	-0.019906	12.17	26.63	22.47	20.42	
C	0.633145	0.453031	-0.003287	0.626160	0.449666	-0.004329	6.99	3.36	1.04	3.80	
H	-0.071771	0.614179	-1.065723	-0.076447	0.605982	-1.073175	4.68	8.20	7.45	6.78	
H	1.051327	0.667269	0.039869	1.02830	0.669417	0.037010	18.50	2.15	2.86	7.83	
H	-0.112169	0.654547	1.027924	-0.116497	0.645966	1.020882	4.33	8.58	7.04	6.65	
C	-0.632855	0.453258	-0.003055	-0.639821	0.449893	-0.004097	6.97	3.37	1.04	3.79	
H	0.109222	0.651562	1.030488	0.104850	0.643009	1.023424	4.37	8.55	7.06	6.66	
H	-1.051506	-0.667741	0.034479	-1.070154	-0.669888	0.031621	18.65	2.15	2.86	7.88	
H	0.074531	0.617105	-1.063167	0.069859	0.608884	-1.070596	4.67	8.22	7.43	6.77	
Total		0.000014	-0.492735	0.000096	-0.081302	-0.563939	-0.059167	81.32	71.20	59.26	70.59

Optimized XYZ coordinates

1W2F

N	-0.2269999	3.3279991	-0.2129999
H	0.0865297	2.3623202	-0.1140098
C	-0.5009999	2.8509992	-2.4549993
C	-0.6139998	3.8139989	-1.3509996
O	-1.0099997	4.9749986	-1.5069996
H	-1.4421796	2.8147348	-3.0151301
H	-0.2291123	1.8383224	-2.1476691
H	0.2594772	3.2064922	-3.1612170
C	-0.2429999	4.1439988	0.9239997
C	1.1769997	4.2509988	1.4179996
O	1.8349995	3.2489991	1.6729995
C	-1.1349997	3.4939990	1.9289995
C	-1.0359997	4.0899989	3.2519991
C	-1.2739996	5.4299985	3.4309990
C	-0.7439998	3.3039991	4.3439988
C	-1.2049997	5.9709983	4.7139987
C	-0.6799998	3.8389989	5.5819984
C	-0.9179997	5.1659986	5.7709984
H	-0.6372234	5.1189725	0.6288597
H	-2.1627802	3.5439619	1.5401926
H	-0.8734850	2.4334400	1.9793550
H	-1.5304919	6.0647978	2.5855896
H	-0.5467622	2.2439528	4.1921071
H	-1.3956244	7.0319194	4.8635884
H	-0.4433805	3.2069385	6.4368405
H	-0.8691368	5.5878428	6.7735868
N	1.6499995	5.4799985	1.5369996
C	3.0469991	5.7269984	1.8469995
H	1.0859962	6.2526537	1.2187147
H	3.3547604	5.0784196	2.6710200
H	3.1729454	6.7726019	2.1396987
H	3.6921046	5.5116692	0.9856480
Se	0.0000000	0.0000000	0.0000000
C	-3.9819989	-3.2929991	2.8189992
C	-2.6449993	-3.3569991	2.1139994
O	-2.4729993	-4.1769988	1.2639996
H	-4.0796245	-2.4944769	3.5651270
H	-4.1552397	-4.2565683	3.3092114
H	-4.7635452	-3.1690072	2.0638725
N	-1.6999995	-2.5119993	2.5049993
C	-0.3809999	-2.5529993	1.9159995
C	0.3289999	-3.8779989	2.0999994
O	1.2229997	-4.1889988	1.3299996
C	0.4969999	-1.4189996	2.4209993
C	0.0780000	-0.0910000	1.9359995
C	-1.9149995	-0.1720000	-0.2419999
H	-1.8949283	-1.8375576	3.2295583
H	-0.4745203	-2.4737004	0.8281936
H	1.5167201	-1.6389399	2.0863732
H	0.5225639	-1.4351131	3.5233833
H	0.7729906	0.6961494	2.2488192
H	-0.9157172	0.1954742	2.3015940
H	-2.4359824	0.6047166	0.3255067
H	-2.2649851	-1.1617122	0.0590626
H	-2.1169711	-0.0287283	-1.3067619
N	-0.1040000	-4.6669987	3.0789991
C	0.5039999	-5.9599983	3.3979990
H	-0.8578638	-4.3461095	3.6652806
H	-0.2775565	-6.7114688	3.5509151
H	1.1263759	-5.8970812	4.2997830
H	1.1310432	-6.2529906	2.5540107

4KRG

N	-0.9549997	-3.1139991	1.6409995
H	-0.9419034	-2.1999664	1.1975223
C	-2.1839994	-3.8569989	-0.3099999
C	-1.6049996	-4.1239988	1.0719997
O	-1.7359995	-5.2249985	1.6069995
H	-1.8290457	-2.9235905	-0.7607901
H	-3.2755989	-3.8161453	-0.2219159
H	-1.9350254	-4.6982184	-0.9622626
C	-0.5589998	-3.1679991	3.0369991
C	-1.8209995	-2.9389992	3.8409989
O	-2.3859993	-1.8379995	3.8319989
C	0.4549999	-2.0779994	3.3659991
O	1.6309995	-2.2499994	2.6069993
H	-0.1256074	-4.1566603	3.2320784
H	0.6504096	-2.0871869	4.4504298
H	0.0348237	-1.1028725	3.1127989
H	2.0117622	-3.1129099	2.8059636
N	-2.2809994	-3.9769989	4.5219987
C	-3.5199990	-3.8569989	5.2649985
H	-1.9568535	-4.8969780	4.2565572
H	-3.4794143	-2.9661264	5.8964538
H	-3.6516486	-4.7438284	5.8905124
H	-4.3838390	-3.7540024	4.5954889
Se	0.0000000	0.0000000	0.0000000
C	-5.1749985	1.4189996	-3.3929990
C	-4.9139986	2.1999994	-2.1029994
O	-5.6359984	3.1379991	-1.7739995
H	-6.2103031	1.0667426	-3.3784388
H	-4.5049864	0.5662678	-3.5515103
H	-5.0776289	2.1074795	-4.2391850
N	-3.8749989	1.7989995	-1.3789996
C	-3.4879990	2.4489993	-0.1310000
C	-3.0379991	3.8939989	-0.3639999
O	-2.9289992	4.6689987	0.5849998
C	-2.3569993	1.6579995	0.5189999
C	-1.1749997	1.5089996	-0.4119999
C	1.0109997	0.8029998	1.4639996
H	-3.4233350	0.9325182	-1.6269657
H	-4.3512272	2.5115778	0.5391112
H	-2.0664528	2.1704704	1.4400052
H	-2.7420073	0.6719598	0.8086998
H	-0.5602188	2.4145979	-0.4298735
H	-1.4666486	1.3249810	-1.4498404
H	1.5447910	1.6827370	1.0952967
H	1.7230118	0.0488197	1.8043687
H	0.3462893	1.0853156	2.2842303
N	-2.7689992	4.2479988	-1.6219995
C	-2.3839993	5.6149984	-1.9739994
H	-2.9492392	3.5987572	-2.3682990
H	-1.7610338	6.0253131	-1.1761153
H	-3.2669309	6.2566178	-2.0868965
H	-1.8241777	5.6008022	-2.9133888

C	1.6604013	0.8421717	0.5904047
O	2.3856485	1.1318510	-0.3508247
N	1.2667569	-0.4409682	0.9116468
H	0.6207759	-0.5253765	1.6921494
C	1.1171410	1.9153533	1.5326021
H	1.9680058	2.4165458	2.0055142
H	0.5899750	2.6648509	0.9336850
H	0.4477207	1.5343644	2.3103075
C	1.5772995	-1.6590283	0.2749215
C	1.1460568	-2.8417797	0.9067342
C	2.2725398	-1.7454854	-0.9439663
C	1.3929103	-4.0845362	0.3281315
C	2.5157620	-3.0000697	-1.5081241
C	2.0803593	-4.1728844	-0.8864396
H	0.6193785	-2.7781251	1.8568937
H	2.6131957	-0.8401395	-1.4279690
H	1.0518554	-4.9858628	0.8321613
H	3.0549879	-3.0548517	-2.4510586
H	2.2770160	-5.1418984	-1.3376464
Se	-1.9444713	-0.8758611	2.4231168
C	-2.5621064	0.9865287	2.1789348
H	-3.5951023	0.9864950	1.8231935
H	-2.5058374	1.4805116	3.1520707
H	-1.9128874	1.4998283	1.4656753
C	-2.0706701	-1.3881006	0.5175486
H	-3.1065406	-1.2984263	0.1825737
H	-1.4118093	-0.7501542	-0.0760151
H	-1.7362347	-2.4244633	0.4375969

NPAA-DMTe

C	1.6372678	0.8256070	0.5852153
O	2.2931933	1.1323443	-0.4002423
N	1.3092093	-0.4688120	0.9362942
H	0.7166599	-0.5678761	1.7557003
C	1.1165084	1.8855228	1.5543703
H	1.9782044	2.3883832	2.0058387
H	0.5659515	2.6360174	0.9787908
H	0.4740708	1.4922999	2.3490368
C	1.6104349	-1.6799384	0.2820453
C	1.2133060	-2.8706360	0.9210277
C	2.2644759	-1.7525209	-0.9603482
C	1.4510298	-4.1074730	0.3263735
C	2.4994707	-3.0013422	-1.5405143
C	2.0958180	-4.1819425	-0.9122383
H	0.7193765	-2.8181358	1.8894703
H	2.5789662	-0.8412064	-1.4506206
H	1.1348609	-5.0147886	0.8358471
H	3.0063821	-3.0449850	-2.5017973
H	2.2837470	-5.1461826	-1.3770723
Te	-2.0608742	-0.9226715	2.5832049
C	-2.6475476	1.1436464	2.2007068
H	-3.6587447	1.1586318	1.7905192
H	-2.6202124	1.6793333	3.1524544
H	-1.9375819	1.5882628	1.5010076
C	-2.0593600	-1.4465010	0.4668556
H	-3.0696144	-1.3332157	0.0702990
H	-1.3531125	-0.7973311	-0.0534028
H	-1.7297617	-2.4839934	0.3849916

2PY-DMSe

N	-1.4396747	0.2222760	-0.2072837
C	-0.4424499	1.2234722	-0.2201145
C	0.8805801	0.7179662	0.0919546
C	1.0973390	-0.6094351	0.3640133
C	0.0312444	-1.5516050	0.3530221
C	-1.2261399	-1.0925199	0.0617845
O	-0.7435793	2.3932416	-0.4808204
H	-2.3943520	0.5375558	-0.4237582
H	1.6870833	1.4442376	0.0977343
H	2.1047634	-0.9525075	0.5933304
H	0.1956828	-2.6013673	0.5664591
H	-2.1046340	-1.7309802	0.0284674
Se	-4.5796299	1.5209296	-0.9874098
C	-3.5743766	2.3384779	-2.4846218
C	-4.0671368	2.8861972	0.3519450
H	-2.5437990	2.4972177	-2.1565144
H	-3.6124398	1.6403533	-3.3248706
H	-4.0444093	3.2842002	-2.7645314
H	-2.9778994	2.9789162	0.3444992
H	-4.5411990	3.8378132	0.1002016
H	-4.4218274	2.5391990	1.3258914

2PY-DMTe

N	-1.4540292	0.1278623	-0.1961088
C	-0.4992746	1.1695738	-0.2245097
C	0.8448048	0.7224645	0.0824009
C	1.1188533	-0.5916076	0.3653673
C	0.0929942	-1.5777072	0.3699895
C	-1.1845135	-1.1750451	0.0831507
O	-0.8474453	2.3241941	-0.4922305
H	-2.4201040	0.4050096	-0.4071831
H	1.6184220	1.4834639	0.0754311
H	2.1410694	-0.8892118	0.5914465
H	0.3031139	-2.6175079	0.5920627
H	-2.0354500	-1.8501484	0.0615077
Te	-4.7868074	1.5374587	-1.0250916
C	-3.5475746	2.3826849	-2.6107115
C	-4.0830658	2.9754533	0.4584139
H	-2.5403647	2.4961709	-2.2035331
H	-3.5556490	1.6806624	-3.4479584
H	-3.9636073	3.3429987	-2.9198336
H	-2.9928978	2.9959923	0.3930693
H	-4.5142288	3.9545964	0.2432485
H	-4.4110891	2.6262748	1.4404529

NMFA-DMSe

C	1.3908733	0.4931803	-0.0390539
O	2.5427429	0.9019145	-0.0439518
N	1.0224903	-0.8112471	-0.0190086
H	0.0314476	-1.0407083	-0.0135773
C	2.0077195	-1.8849646	-0.0007630
H	2.6547341	-1.8323575	-0.8837802
H	2.6465091	-1.8118726	0.8869140
H	1.4835760	-2.8437461	0.0081879
H	0.5095049	1.1755509	-0.0514601
Se	-2.5805415	-1.0683435	0.0503040
C	-2.4054744	0.2576094	1.5073423
H	-3.2438299	0.9572991	1.4700627
H	-2.4269746	-0.2953593	2.4495110
H	-1.4563601	0.7912860	1.4158023
C	-2.5249996	0.2307192	-1.4400196
H	-1.5702302	0.7624289	-1.4377618
H	-2.6282251	-0.3382947	-2.3671577
H	-3.3555230	0.9341576	-1.3439676

NMFA-DMTe

C	1.3993975	0.4860199	-0.0443787
O	2.5439436	0.9143925	-0.0491088
N	1.0544193	-0.8249944	-0.0223360
H	0.0683871	-1.0726960	-0.0172832
C	2.0533494	-1.8854831	-0.0000615
H	2.7012806	-1.8273080	-0.8819126
H	2.6889302	-1.8032581	0.8889464
H	1.5403685	-2.8503544	0.0095541
H	0.5052080	1.1517747	-0.0585146
Te	-2.7391488	-1.1966938	0.0565934
C	-2.4311416	0.2799401	1.6338188
H	-3.2368369	1.0153562	1.6017620
H	-2.4496601	-0.2557221	2.5859119
H	-1.4595136	0.7586067	1.4964309
C	-2.5564032	0.2553856	-1.5622786
H	-1.5759535	0.7328894	-1.5119161
H	-2.6540236	-0.2947126	-2.5013342
H	-3.3551615	0.9941110	-1.4762707

References

- (1) Biswal, H. S.; Chakraborty, S.; Wategaonkar, S. Experimental Evidence of O–H \cdots S Hydrogen Bonding in Supersonic Jet. *J. Chem. Phys.* **2008**, *129*, 184311.
- (2) Biswal, H. S.; Shirhatti, P. R.; Wategaonkar, S. O–H \cdots O versus O–H \cdots S Hydrogen Bonding I: Experimental and Computational Studies on the p-Cresol \cdots H₂O and p-Cresol \cdots H₂S Complexes. *J. Phys. Chem. A* **2009**, *113*, 5633-5643.
- (3) Biswal, H. S.; Wategaonkar, S. Nature of the N–H \cdots S Hydrogen Bond. *J. Phys. Chem. A* **2009**, *113*, 12763-12773.
- (4) Biswal, H. S.; Bhattacharyya, S.; Wategaonkar, S. Molecular-Level Understanding of Ground- and Excited-State O–H \cdots O Hydrogen Bonding Involving the Tyrosine Side Chain: A Combined High-Resolution Laser Spectroscopy and Quantum Chemistry Study. *Chemphyschem* **2013**, *14*, 4165-4176.
- (5) Glendening, E. D.; Landis, C. R.; Weinhold, F. NBO 6.0: Natural Bond Orbital Analysis Program. *J. Comp. Chem.* **2013**, *34*, 1429-1437.
- (6) Contreras-García, J.; Johnson, E. R.; Keinan, S.; Chaudret, R.; Piquemal, J. P.; Beratan, D. N.; Yang, W. NCIPILOT: A Program for Plotting Non-Covalent Interaction Regions. *J. Chem. Theory Comput.* **2011**, *7*, 625-632.
- (7) Frisch, M. J.; Trucks, G. W.; Schlegel, H. B.; Scuseria, G. E.; Robb, M. A.; Cheeseman, J. R.; Montgomery, J. A., Jr.; Vreven, T.; Kudin, K. N.; Burant, J. C.; et al. Gaussian 09, Revision C.01; Gaussian, Inc.: Wallingford, CT, **2011**.
- (8) Furche, F.; Ahlrichs, R.; Hättig, C.; Klopper, W.; Sierka, M.; Weigend, F. Turbomole. *WIREs Comput. Mol. Sci.* **2014**, *4*, 91-100.

- (9) Glendening, E. D.; Landis, C. R.; Weinhold, F. NBO 6.0: Natural Bond Orbital Analysis Program. *J. Comp. Chem.* **2013**, *34*, 1429-1437.
- (10). Word, J. M.; Lovell, S. C.; Richardson, J. S.; Richardson, D. C. Asparagine and Glutamine: Using Hydrogen Atom Contacts in the Choice of Side-Chain Amide Orientation. *J. Mol. Biol.* **1999**, *285*, 1735-1747.